Special issue of the 2nd International Conference on Computational and Experimental Science and Engineering (ICCESEN 2015)

Identification of Structural and Spectral Features of 2-Amino 4-Chlorobenzoic Acid and 4-Amino 2-Chlorobenzoic Acid: A Comparative Experimental and DFT Study

N. Kaya Kinaytürk[a] and H. Oturak[b*]

[a]Süleyman Demirel University, Experimental and Observational Research and Application Centre, Isparta, Turkey
[2]Süleyman Demirel University, Physics Department, Isparta, Turkey

The structure and spectroscopic data of the molecules in the ground state were calculated using density functional theory employing B3LYP/6–311++G(d,p) basis set. The dipol moment, linear polarizability and first hyperpolarizability values were also computed using the same basis set. A study on the electronic properties, such as HOMO-LUMO energies, were performed by time-dependent density functional theory approach. A detailed description of spectroscopic behaviour of compounds was given based on the comparison of experimental data and theoretical computations.

DOI: 10.12693/APhysPolA.130.276

PACS/topics: 31.15.E, 33.20.Lg, 33.20.Ea

1. Introduction

The molecular prototype of an aromatic carboxylic acid is benzoic acid (BA). It is the simplest aromatic carboxylic acid, and it is also one of the most important acids in chemistry [1]. Derivatives of benzoic acid have been the subject of investigation for many reasons. Derivative of benzoic acid is an essential component of the vitamin complex [2]. 2-Aminobenzoic acid is known as vitamin L, whereas 4-Aminobenzoic acid is known as vitamin B and bacterial vitamin H. Vitamin B complex is a group of water-soluble substances including possible 4-Aminobenzoic acid, which is known as antibacterial agent [3]. Vitamin B complex is used in miticides, contrast media in urology, cholecystographic examinations and in the manufacture of pharmaceuticals [4, 5]. Therefore, BA and derivatives have been the subject of several studies the last three decades.

Experimental and theoretical quantum chemical studies of benzoic acid and of the substituted benzoic acids have been carried out by various researches. The geometric parameters and vibrational wavenumbers of benzoic acid have been recorded in [1]. The crystal structure of 2-Amino-4-Chlorobenzoic acid (2A4ClBA) [6] and 4-Amino-2-Chlorobenzoic acid (4A2ClBA) [7] were published. A detailed structural analysis of 2-Amino-5-Chlorobenzoic acid was carried out by Karabacak and Çınar [8]. Samsonowicz et al. have recorded the effect of amino group substituted at 2-, 3-, 4-position of benzoic acid [3]. Sundaragenasan et al. [2, 4, 9, 10] have recorded the FT-IR and FT-Raman spectra of 2-Amino-4,5-difluorobenzoic acid, 5-Amino-2-Chlorobenzoic acid, 5-Amino-2-nitrobenzoicacid and 2-Chlorobenzoic acid.

*corresponding author; e-mail: haliloturak@sdu.edu.tr

The aim of this paper was to determine the geometry and theoretical spectroscopic (FT-IR, FT-Raman, ^{1}H and ^{13}C-NMR, UV-Vis) structures of 2A4ClBA and 4A2ClBA and to compare them with experimental data. In addition, HOMO and LUMO energies of title molecules are presented.

2. Experimental details

The compounds of 2A4ClBA and 4A2ClBA in solid form were purchased from Sigma-Aldrich chemical company (U.S.A.) with a stated purity of greater than 98%, and were used as such without further purification. The FT-IR spectrum was recorded using KBr pellets on a Perkin Elmer Spectrum BX FTIR spectrophotometer in the region of 4000–400 cm^{-1}. The FT-Raman spectrum was obtained on a DXR-Raman microscope in the region of 3500–12 cm^{-1}. The ^{1}H and ^{13}C NMR were taken in DMSO solutions on a Bruker Ultrashield 400 Plus NMR spectrometer. Proton and carbon signals were referenced to TMS. UV-Visible analyses were carried out with a Perkin Elmer Lambda 20 Spectrophotometer. All spectra were measured at room temperature.

3. Computational details

Gaussian 09 [11] software package was used for the theoretical calculations. The quantum chemical calculations were performed applying the density functional theory (DFT) method, with the B3LYP functional and the 6–311G++(d,p) basis set. Since B3LYP vibrational wavenumbers are known to be higher than the experimental wavenumbers, as a result of the neglected anharmonicity effects [12], they were scaled down by a uniform scaling factor of 0.983 for wavenumbers up to 1700 cm^{-1} and of 0.958 for wavenumbers greater than 1700 cm^{-1} [13]. The scaled wavenumbers, in general,

show good agreement with experimental ones. The geometry optimizations were followed by frequency calculations using the same basis set. Also, the same basis set and functional was used for the ^{1}H and ^{13}C NMR shielding constants calculations by applying the GIAO (gauge-including atomic orbital) method. UV-Vis spectra and electronic properties were determined by time-dependent DFT (TD-DFT). The results were visualized using Gauss View program [14]. Total energy distribution, corresponding to the observed frequencies, was calculated using VEDA 4 program [15].

4. Results and discussion

4.1. Molecular geometry

The optimized molecular structures of 2A4ClBA and 4A2ClBA, calculated using DFT theory at B3LYP/6–311++G(d,p) level are shown in Fig. 1a and b. Experimental crystal geometry for the title compounds has been reported by Farag et al. [6] and Khan [7]. The geometrical parameters, such as bond length, bond angle and dihedral angles, are compared with the x-ray data of title compounds, shown in Table I. The optimized and experimental crystal structure shows significant degree of agreement.

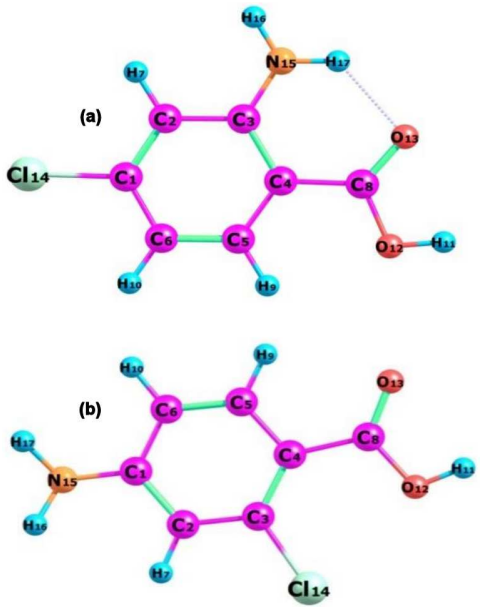

Fig. 1. The theoretical geometric structure of (a) 2A4ClBA and (b) 4A2ClBA.

4.2. Conformer analysis

The structure of the molecules, with numbering scheme for the atoms and torsion angles, is presented in Fig. 1a and b. We have performed the potential energy surface analysis on the rotations θ (C5-C4-C8-O12) and ϕ (C4-C8-O12-H11) torsion angles, scanning from $-180°$ to 180° in steps of 10°. Potential energy surface scan studies have been carried out by DFT calculations using 6–31G(d) basis set (Fig. 2a and b) for both molecules. Basis set 6–31G(d) was used because there were some computational errors in high sets. The most stable conformers were obtained with the energy of −935.7790 a.u. (−25463.85 eV), and with the torsion angles of 180° (ω) and 180° (φ) for 2A4ClBA and −935.7650 a.u. (−25463.47 eV), and with the torsion angles of 180° (ω) and 180° (φ) for 4A2ClBA, respectively. The computational processes were then followed by the geometry optimization, carried out using DFT/B3LYP/6–311++G(d,p) level of theory. The energy of the most stable conformer and dihedral angles (θ, ϕ) were found to be −935.9545 a.u. (25468.63 eV) and −935.9409 a.u. (25468.26 eV) and 0.8906°, −179.80° and −179.02°, 179.93°, respectively.

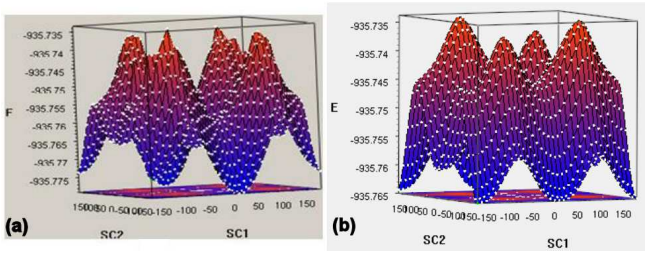

Fig. 2. The potential energy surface scan for (a) 2A4ClBA and (b) 4A2ClBA.

4.3. Vibration analysis

4.3.1. C–H vibrations

The characteristic C–H bands in aromatic compounds are investigated in three distinctive regions [16]. The asymmetric and symmetric C–H stretching bands appear in the 3100–3000 cm^{-1} range, the in-plane C–H stretching bands in the 1275–1000 cm^{-1} and the out-of-plane C–H stretching bands in the 900–650 cm^{-1} range [16, 17]. As a result of the theoretical calculation of vibrational frequencies of 2A4ClBA molecule, the 3115 cm^{-1} [$\nu_{CH}(97)$], 3131 cm^{-1} [$\nu_{CH}(96)$], 3145 cm^{-1} [$\nu_{CH}(93)$] range was assigned to C–H stretching bands, the 1256 cm^{-1} [$\delta_{HCC}(66)$] to the in-plane C–H stretching bands and 754 cm^{-1} [$\tau_{HCCC}(70)$] and 823 cm^{-1} [$\tau_{HCCC}(50)$] to the out-of-plane C–H stretching bands. Regarding the experimental results, while the C–H stretching bands appeared in the 2945–3000–3057 cm^{-1} range in the IR spectrum, in-plane and out-of-plane C–H stretching bands were observed in the 1315 and 760–849 cm^{-1} ranges, respectively. Similarly, the corresponding bands of 4A2ClBA molecule were theoretically assigned to 3116 cm^{-1} [$\nu_{CH}(100)$], 3134 cm^{-1} [$\nu_{CH}(97)$], 3151 cm^{-1} [$\nu_{CH}(94)$], 1112 cm^{-1} [$\delta_{HCC}(66)$], 1219 cm^{-1} [$\delta_{HCC}(47)$], and 805 cm^{-1} [$\tau_{HCCN}(62)$], 821 cm^{-1} [$\tau_{HCCN}(71)$], 949 cm^{-1} [$\tau_{HCCC}(79)$], respectively. In the experimental IR spectrum, C–H stretching bands, in-plane stretching bands and out-of-plane stretching bands were observed in the 2808–2865–2987 cm^{-1}, 1137–1244 cm^{-1} and 789–847–965 cm^{-1} ranges, respectively.

4.3.2. C–NH_2 vibrations

The scaled –NH_2 symmetric and asymmetric stretches in the range of 3529–3695 cm^{-1} are in agreement with experimental symmetric and asymmetric stretching at 3338 and 3210 cm^{-1} for 4A2ClBA. The calculated –NH_2 scissoring vibrations at 1577 cm^{-1} [$\delta_{HNH}(56)$] and 1594 cm^{-1} [$\delta_{HNH}(67)$] for title molecules is in excellent agreement with expected characteristic value, 1620 cm^{-1}. This is also in excellent agreement with the recorded medium strong band in FT-IR at 1585 and 1597 cm^{-1} for 2A4ClBA and 4A2ClBA, respectively. The C–NH_2 out of plane and in plane bending vibrations are at 191 cm^{-1} [$\tau_{HNCC}(20)$], 388 cm^{-1} [$\delta_{NCC}(42)$], for 2A4ClBA and 401 cm^{-1} [$\tau_{HNCC}(96)$], 271 cm^{-1} [$\delta_{NCC}(20)$], for 4A2ClBA, respectively.

4.3.3. –COOH group vibrations

The vibrational bands of the COOH groups contain the C–O, C=O and O–H vibrational modes [18, 19]. C=O stretching band appears strongly in the region of 1870–1540 cm^{-1}. As a result of the theoretical calculation, 1644 cm^{-1} [$\nu_{OC}(68)$], and 1683 cm^{-1} [$\nu_{OC}(81)$] vibration energies were assigned to 2A4ClBA and 4A2ClBA molecules, respectively. Experimental IR spectra have revealed that this band appears at 1666 and 1670 cm^{-1}. The stretching band of –OH hydroxyl group appears approximately at 3600 cm^{-1}. It was calculated to be at 3626 cm^{-1} [$\nu_{OH}(100)$], and 3695 cm^{-1} [$\nu_{OH}(100)$] for 2A4ClBA and 4A2ClBA molecules respectively and at 3501 and 3425 cm^{-1} in the experimental IR spectra.

4.3.4. C–C ring vibrations

C–C ring stretches in aromatic compounds appear in the 1600–1400 cm^{-1} region [20, 21]. In this study, according to the calculation based on DFT-B3LYP–6311++G(d,p) basis set, ring stretches were assigned to 1549 cm^{-1} [$\nu_{CC}(32)$], 1502 cm^{-1} [$\nu_{CC}(43)$], 1328 cm^{-1} [$\nu_{CC}(21)$], 1298 cm^{-1} [$\nu_{CC}(33)$], 1246 cm^{-1} [$\nu_{CC}(24)$], 1071 cm^{-1} [$\nu_{CC}(35)$], 1016 cm^{-1} [$\nu_{CC}(22)$] for 2A4ClBA molecule and 1572 cm^{-1} [$\nu_{CC}(41)$], 1519 cm^{-1} [$\nu_{CC}(59)$], 1395 cm^{-1} [$\nu_{CC}(43)$], 1285 cm^{-1} [$\nu_{CC}(38)$], 1274 cm^{-1} [$\nu_{CC}(47)$], 879 cm^{-1} [$\nu_{CC}(63)$] for 4A2ClBA molecule. The 2A4ClBA molecule appeared at 1585, 1550, 1344, 1249, 1097 cm^{-1} in the IR spectrum and 1553, 1333, 1243, 1101, 731 cm^{-1} in the Raman spectrum. The 4A2ClBA molecule was observed at 1597, 1500, 1405, 1286, 911 cm^{-1} in the IR spectrum and at 1598, 1460, 1321, 913 cm^{-1} in the Raman spectrum. In-plane and out-of-plane C–C stretches are a characteristic region for ring vibrations [22]. These vibrations frequently overlap with C–O–C, O–C–C vibrations. In the present study, in-plane and out-of-plane ring stretches, which were observed at the 208, 301 and 498 cm^{-1} for 2A4ClBA molecule have overlapped with O–C–C stretches. The same was observed for the 4A2ClBA molecule. The comparison of data obtained for both molecules reveals that C–C vibration bands of 4A2ClBA are shifted to high frequency region.

4.3.5. C–Cl Vibrations

When C–Cl stretching, in-plane and out-of-plane bending vibrations were assigned, they were compared with those of similar molecules as 2-Chlorobenzoic acid [10], p-Chlorobenzoic acid [21], 5-Amino-2-Chlorobenzoic acid [9] and 2-Amino-5-Chlorobenzoic acid [8]. Shurvell [16] and Stuart [23] have assigned C–X group (X=Cl, Br, I) stretching vibrations to the 800–550 cm^{-1} range. On the other hand, Mooney [24, 25] has assigned them to the 1129–480 cm^{-1} region. In the current study, these stretching vibrations were calculated to be 356 cm^{-1} [$\nu_{ClC}(11)$], 498 cm^{-1} [$\nu_{ClC}(24)$], 691 cm^{-1} [$\nu_{ClC}(12)$], 924 cm^{-1} [$\nu_{ClC}(17)$] for 2A4ClBA, and 316 cm^{-1} [$\nu_{ClC}(12)$], 401 cm^{-1} [$\nu_{ClC}(32)$], 673 cm^{-1} [$\nu_{ClC}(10)$], 879 cm^{-1} [$\nu_{ClC}(19)$] for 4A2ClBA. While C–Cl in-plane stretching vibrations for 2A4ClBA were calculated to be at 194 [$\delta_{ClCC}(34)$], and 307 cm^{-1} [$\delta_{ClCC}(11)$], they were observed at 208 and 301 cm^{-1} in the Raman spectrum. Vibrations calculated to be at 440 cm^{-1} [$\tau_{ClCCC}(15)$], 600 cm^{-1} [$\tau_{ClCCC}(23)$] and 171 cm^{-1} [$\tau_{ClCCC}(39)$], 520 cm^{-1} [$\tau_{ClCCC}(26)$] for these molecules were assigned as out-of-plane C-Cl stretches. The theoretical data, related literature and experimental data seem to be overlapping.

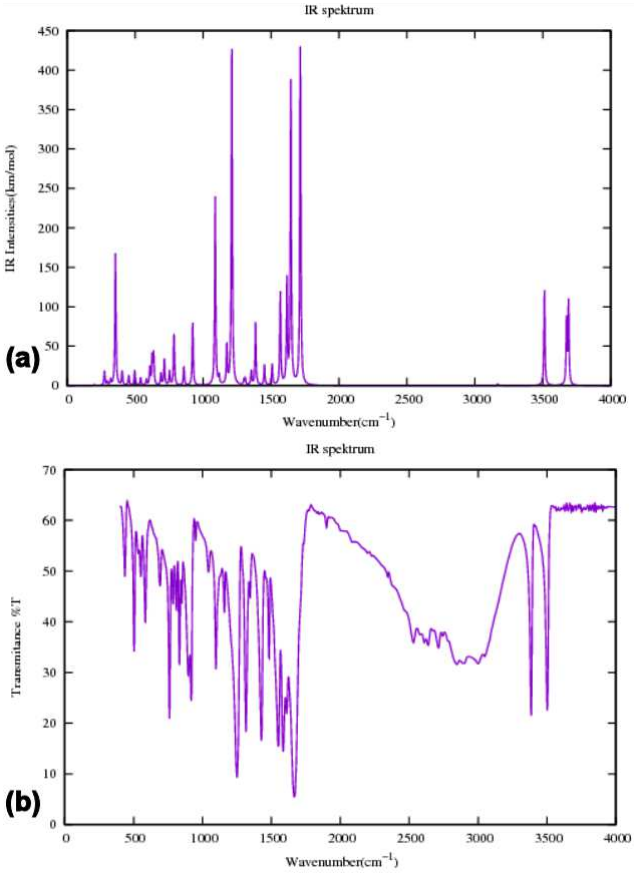

Fig. 3. The calculated (a) and experimental (b) infrared spectra of 2A4ClBA.

TABLE I

Optimized parameters for 2A4ClBA and 4A2ClBA (bond length, bond angles and dihedral angles).

2-Amino 4-Chlorobenzoic acid			4-Amino 2-Chlorobenzoic acid		
Parameters	x-ray	B3LYP 6311++G(d,p)	Parameters	x-ray	B3LYP 6311++G(d,p)
Bond lengths					
Cl14-C1	1.7425	1.7764	Cl14-C3	1.732	1.7555
O13-C8	1.2415	1.2217	O13-C8	1.226	1.2134
O12-C8	1.3197	1.3577	O12-C8	1.3513	1.302
O12-H11	0.854	0.9681	O12-H11	0.82	0.9691
N15-C3	0.3572	1.3598	N15-C1	1.386	1.3801
N15-H16	0.851	1.0050	N15-H16	0.85	1.008
N15-H17	0.826	1.0108	N15-H17	0.86	1.008
C1-C6	1.3933	1.3995	C1-C6	1.39	1.4061
C1-C2	1.3746	1.3789	C1-C2	1.392	1.4019
C6-H10	0.9300	1.0809	C6-H10	0.93	1.083
C6-C5	1.3816	1.3814	C6-C5	1.37	1.3784
C5-H9	0.9300	1.0817	C5-H9	0.93	1.083
C5-C4	1.4078	1.4066	C5-C4	1.4087	1.40
C4-C8	1.4651	1.4657	C4-C8	1.47	1.4853
C4-C3	1.4185	1.4259	C4-C3	1.398	1.4093
C3-C2	1.4093	1.4129	C3-C2	1.383	1.3889
C2-H7	0.9300	1.0831	C2-C7	0.93	1.083
Bond angles [°]					
C8-O12-H11	107.8(11)	106.3513	C8-O12-H11	108(2)	105.91
C3-N15-H16	123.2(10)	120.0303	C1-N15-H16	117.7(19)	117.70
C3-N15-H17	117.9(12)	118.8416	C1-N15-H17	117(2)	118
Cl14-C1-C6	118.99(5)	118.88	Cl14-C3-C2	115.19(18)	115.0638
Cl14-C1-C2	118.00(5)	118.80	Cl14-C3-C4	123.03(18)	123.6495
C2-C3-C4	118.28(6)	118.19	C2-C3-C4	121.8(2)	121.2863
C3-C2-C1	119.92(6)	120.3082	C3-C2-C1	120.3(2)	121.0909
C2-C1-C6	123.01(6)	122.3161	C2-C1-C6	119.0(2)	118.3761
N15-C3-C4	123.17(6)	122.3078	N15-C1-C6	120.8(2)	121.0098
N15-C3-C2	118.55(6)	119.4932	N15-C1-C2	120.2(2)	120.5738
C1-C6-C5	117.38(6)	117.7394	C1-C6-C5	120.0(2)	119.8603
C6-C5-C4	121.95(7)	122.2169	C6-C5-C4	122.5(2)	122.9419
C5-C4-C8	119.34(6)	120.4702	C5-C4-C8	118.9(2)	114.9140
C3-C4-C8	121.20(6)	120.3033	C3-C4-C8	124.5(2)	128.6415
C3-C4-C5	119.45(6)	119.2248	C3-C4-C5	116.5(2)	116.4443
O13-C8-C4	123.38(7)	125.8351	O13-C8-C4	123.8(2)	123.3375
O12-C8-C4	114.92(6)	113.8652	O12-C8-C4	114.0(2)	115.5287
O12-C8-O13	121.70(7)	120.2996	O12-C8-O13	122.1(2)	121.1337
C3-C2-H7	120.0	120.1017	C3-C2-H7	120	118.9112
C1-C2-H7	120.0	120.3082	C1-C2-H7	120	119.9956
H16-N15-H17	117.7(15)	120.2671	H16-N15-H17	112(3)	114.44
Dihedral angles [°]					
N15-C3-C2-C1	178.90(7)	179.0249	N15-C1-C2-C3	-180.0(2)	177.7497
C4-C3-C2-C1	-1.19(11)	-0.17	C4-C3-C2-C1	1.1(3)	0.00306
C3-C2-C1-C6	0.96(12)	-0.0447	C3-C2-C1-C6	-2.5(3)	0.03625
C3-C2-C1-Cl14	-177.87(6)	-179.9959	C1-C2-C3-Cl14	179.44(17)	179.7966
C2-C1-C4-C5	-0.05(12)	-0.1448	C2-C3-C4-C5	0.4(3)	0.0157
Cl14-C1-C4-C5	178.77(6)	-179.9041	Cl14-C3-C4-C5	-179.00(17)	-179.7597
C1-C6-C5-C4	-0.59(12)	-0.0256	C1-C6-C5-C4	-1.0(4)	0.1204
C6-C5-C4-C3	0.33(11)	-0.025	C6-C5-C4-C3	-0.5(3)	-0.07835
C6-C5-C4-C8	-178.31(7)	179.3565	C6-C5-C4-C8	176.5(2)	179.99
N15-C3-C4-C5	-179.53(8)	-178.8900	N15-C1-C6-C5	179.9(2)	-177.7988
C2-C3-C4-C5	0.57(11)	0.2810	C2-C1-C6-C5	2.5(3)	-0.0957
N15-C3-C4-C8	-0.92(12)	1.5652			
C2-C3-C4-C8	179.18(7)	-179.2637	C2-C3-C4-C8	-176.4(2)	179.9363
C5-C4-C8-O13	174.64(7)	-179.9569	C5-C4-C8-O13	-172.3(2)	-179.0213
C3-C4-C8-O13	-3.97(12)	0.5821	C3-C4-C8-O13	4.4(4)	1.05712
C5-C4-C8-O12	-5.06(11)	0.8907	C5-C4-C8-O12	7.8(3)	0.8792
C3-C4-C8-O12	176.34(7)	-179.5703	C3-C4-C8-O12	-175.4(2)	-179.0424

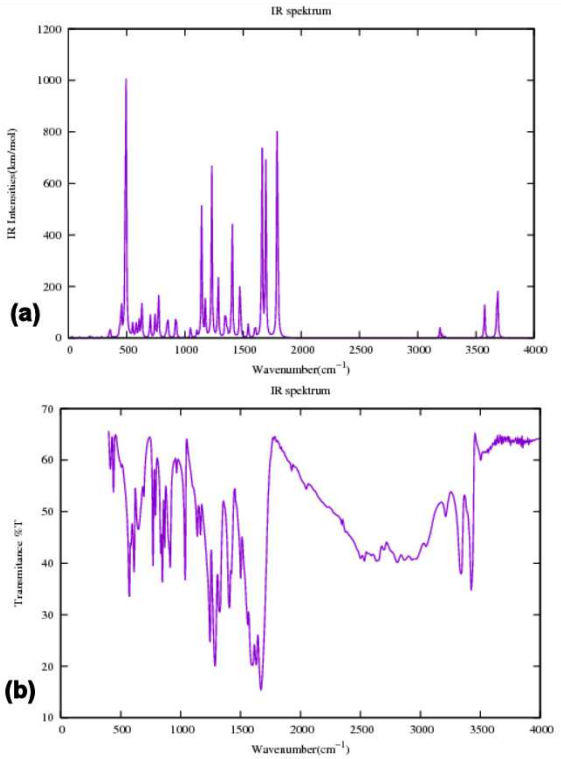

Fig. 4. The calculated (a) and experimental (b) infrared spectra of 4A2ClBA.

4.4. NMR analysis

The ^{13}C and ^{1}H theoretical and experimental chemical shifts and the assignments of 2A4ClBA and 4A2ClBA are shown in Table II. In recent years, GIAO computational method has became efficient in predicting chemical shifts of various organic compounds [26]. In this study, the optimized structures of 2A4ClBA and 4A2ClBA are used to calculate the NMR spectra using the DFT/B3LYP method with 6–311++G(d,p) level using the GIAO method. The result in Table II shows that the range of ^{13}C NMR chemical shift of the typical organic molecule usually is > 100 ppm, which ensures reliable interpretation of spectroscopic parameters [27, 28]. In this study, ^{13}C NMR chemical shifts in the ring for the title molecules are > 100 ppm, as expected. When structures of molecules are searched the peak of carbon is seemed in downfield. A nearby electronegative atom withdraws electron density from the neighbourhood of the proton, so NMR signal of such deshielded proton will appear downfield [29]. Chemical shifts that belong to C(8) are the lowest of other atom in the molecules, because of the oxygen being more electronegative compared with nitrogen and chlorine. The agreement between the experimental and theoretical chemical shifts in ^{13}C and ^{1}H NMR spectra is very good.

TABLE II

Experimental and theoretical ^{13}C and ^{1}H NMR isotropic chemical shifts of 2A4ClBA and 4A2ClBA with DFT (B3LYP 6–311++G(d,p)) method.

	B3LYP 6311++G(d,p) [ppm]		Experimental	
ATOM	2A4ClBA	4A2ClBA	2A4ClBA	4A2ClBA
C(1)	157.81	157.58	138.32	153.09
C(2)	118.72	121.14	114.74	114.99
C(3)	159.07	157.21	152.37	134.83
C(4)	110.56	120.76	108.58	114.61
C(5)	140	142.45	133.01	133.80
C(6)	121.12	114.74	115.11	111.51
C(8)	174.6	168.64	168.90	166
H(7)	6.56	6.66	6.85	6.66
H(9)	7.99	8.24	7.72	7.70
H(10)	6.51	6.49	6.84	6.54
H(11)	5.53	5.40	6.50	6.01
H(16)	4.12	3.55	6.48	2.52
H(17)	7.7	3.54	7.7	2.51

4.5. UV-Vis studies

On the basis of fully optimized ground-state structure, the TD-DFT-B3LYP–6311++G(d,p) method was used to determine the low-lying excited states of 2A4ClBA and 4A2ClBA. The calculated excitation energies, oscillator strength f and wavelength λ and spectral assignments were carried out and the results were compared with measured experimental wavelengths given in Table III. According to the calculation results, three sharp electronic transitions were observed fort title molecules (335, 256, 245 nm for 2A4ClBA in chloroform and 294, 279, 252 nm for 4A2ClBA in dichloromethane) in good agreement with the measured experimental data. According to Franck-Condon principle, the maximum absorption peaks correspond in an UV-Visible spectrum to a vertical excitation [30].

TABLE III

Experimental and theoretical (TD-DFT/B3LYP/6–311++G(d,p)) absorption wavelengths λ [nm] and excitation energies.

$\lambda_{cal.}$	$\lambda_{exp.}$	E [eV]	Assign.	Major contribution
2A4ClBA				
245	240	5.0632	$\sigma \rightarrow \pi^*$	HOMO-2→LUMO
256	253	4.8372	$\pi \rightarrow \pi^*$	HOMO-1→LUMO
335	336	3.6954	$\pi \rightarrow \pi^*$	HOMO→LUMO
4A2ClBA				
252	229	4.9148	$\sigma \rightarrow \pi^*$	HOMO→LUMO
279	279	4.4386	$\sigma \rightarrow \pi^*$	HOMO→LUMO+1
294		4.2132	$\pi \rightarrow \pi^*$	HOMO-2→LUMO

In most cases the application of absorption spectroscopy to organic compounds is based on transitions for σ or π electrons to the π^* excited state, because the energies required for these processes bring the absorption peaks into an experimentally convenient spectral region (200 to 700 nm). The molar absorptivities for peaks associated with excitation of the $\sigma \rightarrow \pi^*$ transitions are generally low and ordinarily range from 10 to 100 l cm^{-1}; values for $\pi \rightarrow \pi^*$ transitions, on the other hand, normally fall in the range between 1000 and 10000 l cm^{-1} [31].

The most important orbitals in molecule are the frontier molecular orbitals, called highest occupied molecular orbital (HOMO) and lowest unoccupied molecular orbital (LUMO). The calculated energy value of HOMO is −0.22892 and −0.22640 eV, for 2A4ClBA and 4A2ClBA, respectively. LUMO is −0.07376 and −0.06734 eV, for 2A4ClBA and 4A2ClBA, respectively. The value of energy separation between the HOMO and LUMO are −0.1556 and −0.15906 eV, for 2A4ClBA and 4A2ClBA, respectively.

Acknowledgments

This work was supported by a grant (Project No: 3656-D2-13) from the Suleyman Demirel University Scientific Research fund.

References

[1] M. Alcolea Palafox, J.L. Nunez, M. Gıl, *Int. J. Quantum Chem.* **89**, 1 (2002).

[2] N. Sundaraganesan, S. Ilakiamani, B.D. Joshua, *Spectrochim. Acta Part A* **67**, 287 (2007).

[3] M. Samsonowicz, T. Hrynaszkiewicz, R. Świsłocka, E. Regulska, W. Lewandowski, *J. Mol. Struct.* **744–747**, 345 (2005).

[4] N. Sundaraganesan, B.D. Joshua, K. Settu, *Spectrochim. Acta Part A* **66**, 2 (2007).

[5] A. Syahrani, E. Ratnasari, G. Indrayanto, A.L. Wilkins, *Phytochemistry* **51**, 615 (1999).

[6] A.M. Farag, S.G. Teoh, H. Osman, C.S. Yeap, H.-K. Fun, *Acta Crystallograph. E* **67**, o37 (2010).

[7] M.H. Khan, I.U. Khan, M. Akkurt, *Acta Crystallograph E* **67**, o2247 (2011).

[8] M. Karabacak, M. Çınar, *Spectrochim. Acta Part A* **86**, 590 (2012).

[9] M. Ramalingam, N. Sundaraganesan, H. Saleem, J. Swaminathan, *Spectrochim. Acta Part A* **71**, 23 (2008).

[10] N. Sundaraganesan, D.B. Joshua, T. Radjakoumar, *Indian J. Pure App. Phys.* **47**, 248 (2009).

[11] M.J. Frisch, G.W. Trucks, H.B. Schlegel, G.E. Suzerain, M.A. Robb, J.R. Cheeseman Jr., J.A. Montgomery, T. Vreven, K.N. Kudin, J.C. Burant, J.M. Millam, S.S. Iyengar, J. Tomasi, V. Barone, B. Mennucci, M. Cossi, G. Scalmani, N. Rega, G.A. Petersson, H. Nakatsuji, M. Hada, M. Ehara, K. Toyota, R. Fukuda, J. Hasegawa, M. Ishida, T. Nakajima, Y. Honda, O. Kitao, H. Nakai, M. Klene, X. Li, J.E. Knox, H.P. Hratchian, J.B. Cross, V. Bakken, C. Adamo, J. Jaramillo, R. Gomperts, R.E. Stratmann, O. Yazyev, A.J. Austin, R. Cammi, C. Pomelli, J.W. Ochterski, P.Y. Ayala, K. Morokuma, G.A. Voth, P. Salvador, J.J. Dannenberg, V.G. Zakrzewski, S. Dapprich, A.D. Daniels, M.C. Strain, O. Farkas, D.K. Malick, A.D. Rabuck, K. Raghavachari, J.B. Foresman, J.V. Ortiz, Q. Cui, A.G. Baboul, S. Clifford, J. Cioslowski, B. Stefanov, G. Liu, A. Liashenko, P. Piskorz, I. Komaromi, R.L. Martin, D.J. Fox, T. Keith, M.A. Al-Laham, C.Y. Peng, A. Nanayakkara, M. Challacombe, P.M.W. Gill, B. Johnson, W. Chen, M.W. Wong, C. Gonzalez, J.A. Pople, Gaussian 09, Gaussian Inc., Pittsburgh 2003.

[12] L. Sinha, O. Prasad, M. Karabacak, H.N. Mishra, V. Narayan, A.M. Asiri, *Spectrochim. Acta Part A* **120**, 126 (2014).

[13] N. Sundaraganesan, S. Ilakiamani, H. Saleem, P.M. Wojciechowski, D. Michalska, *Spectrochim. Acta Part A* **61**, 2995 (2005).

[14] R. Dennington, T. Keith, J. Millam, Gaussview Version 5. s.l., Semichem Inc. Shawnee Mission, KS, (2009).

[15] MH. Jamroz, *Vibrational energy distribution analysis VEDA 4*, 2004.

[16] H.F. Shurvell, *Spectra-Structure Correlations in the Mid- and Far- infrared* in: *Handbook of Vibrational Spectroscopy*, Eds. J.E. Bertie, J.M. Chalmers, P.R. Griffiths, John Wiley & Sons, 2002.

[17] B. Schrader, *Infrared and Raman Spectroscopy Method and Aplication*, John Wiley & Sons, 1995.

[18] M. Karabacak, Z. Cinar, M. Kurt, S. Sudha, N. Sundaraganesan, *Spectrochim. Acta Part A* **85**, 179 (2012).

[19] M. Ibrahim, A. Nada, D.E. Kamal, *Indian J. Pure App. Phys.* **43**, 917 (2005).

[20] P.R. Griffiths, J.A. Haseth, *Fourier Transform Infrared Spectrimetry*, John Wiley & Sons, 2007, p. 447.

[21] N. Sundaraganesan, B. Anand, C. Meganathan, B.D. Joshua, *Spectrochim. Acta Part A* **69**, 871 (2008).

[22] V. Balachandran, S. Lalitha, S. Rajeswari, V.K. Rastogic, *Spectrochimica Acta Part A* **121**, 575 (2014).

[23] B.H. Stuart, *Infrared Spectroscopy: Fundamental and Applications. s.l.*, John Wiley & Sons, 2004, s. 82.

[24] E.F. Mooney, *Spectrochim. Acta* **19**, 877 (1963).

[25] E.F. Mooney, *Spectrochim. Acta* **20**, 1021 (1964).

[26] A.R. Katritzky, N.G. Akhmedov, J. Doskocz, P.P. Mohapatra, C.D. Hall, A. Güven, *Magn. Reson. Chem.* **45**, 532 (2007).

[27] D. Shoba, S. Periandi, S. Boomadevi, S. Ramalingam, E. Fereyduni, *Spectrochim. Acta Part A* **118**, 438 (2014).

[28] M. Karabacak, Z. Cinar, M. Kurt, S. Sudha, N. Sundaraganesan, *Spectrochim. Acta Part A* **85**, 179 (2012).

[29] D. Shoba, S. Periandi, S. Boomadevi, S. Ramalingam, E. Fereyduni, *Spectrochim. Acta Part A* **118**, 438 (2014).

[30] L.D.S. Yadav, *Organic Spectroscopy*, Springer-Science + Business Media, B.V., Allahabat 2005.

[31] D.A. Skoog, D.M. West, *Principles of Instrumental Analysis*, Saunders College, 1980, p. 172.